Pergamon

Journal of Structural Geology, Vol. 18, No. 1, pp. 61 to 73, 1996

0191-8141/96 $15.00+0.00

0191-8141(95)00080-1

Structural and metamorphic evidence of local extension along the Vivero fault coeval with bulk crustal shortening in the Variscan chain (NW Spain)

F. J. MARTÍNEZ, J. CARRERAS and M. L. ARBOLEYA

Departament de Geologia, Universitat Autonoma de Barcelona, 08193 Bellaterra, Spain

and

C. DIETSCH

Department of Geology, University of Cincinnati, Cincinnati, OH 45221-0013, U.S.A.

(*Received* 19 *July* 1994; *accepted in revised form* 7 *July* 1995)

Abstract—The Vivero fault is a W-dipping, N–S-striking ductile shear zone separating the Ollo de Sapo antiform in its western hangingwall and the Lugo dome in its eastern footwall. Two stages of deformation (F_1 and F_2) produced nearly coaxial folds with sub-horizontal axes. A crenulation cleavage S_2 transposes an older S_1. Three sets of shear bands in the hangingwall define a pervasive fabric consistent with an E–W bulk shortening perpendicular to a composite S_{1-2} foliation and NNE-stretching parallel to L_2. The Vivero fault zone is marked by a mylonitic foliation with a steeply NW-plunging stretching lineation and extensional crenulation cleavage (ECC) indicating normal slip. In the vicinity of the fault, sub-horizontal NNE-trending F_3 folds, with a crenulation cleavage S_3, deform earlier-formed fabrics, including a mylonitic foliation.

Pressure–temperature conditions obtained from mineral assemblages on both sides of the Vivero fault yield a minimum throw of 5.5 km. Andalusite-bearing pelite in the hangingwall was infolded by an F_2 synform into the kyanite field at 450–500°C. The eastern edge of these rocks was later accreted to the footwall and heated to andalusite–staurolite conditions at ~600°C.

Slip on the Vivero and Valdoviño faults is kinematically related. East–west shortening during F_2 involved folding and sinistral strike-slip on the Valdoviño fault which induced local extension along the newly generated Vivero fault. Synkinematic emplacement of granitoids along the Vivero fault is favoured by extension. Coeval slip on both faults took place during the later stages of F_2 folding. Geometrical constraints caused northwards escape of the crustal block bounded by the Valdoviño and Vivero faults, recorded by NNE-stretching defined by L_2.

INTRODUCTION

Regional transpressional and transtensional faults play a central role in the structural evolution of many orogenic belts. Since the 1980s, extensional ductile shear zones have been increasingly recognized in orogenic belts and have highlighted the role of extension during orogenesis. In the Variscan chain of Europe, for example, much of the deformation in Brittany is related to movement along the transcurrent South Armorican shear zone (Berthé *et al.* 1979). In the Iberian branch of the Ibero-Armorican arc, Matte (1968) drew attention to the importance of the Vivero fault (Fig. 1) interpreting it and the related structures as due to normal faulting. Ponce de León & Choukroune (1980) recognized another main fault in NW Spain, the Valdoviño fault (Fig. 1), as a major ductile sinistral strike-slip fault zone, and established that relationships between fault movement and folding are similar to those in Brittany (Berthé & Brun 1980). Ponce de León and Choukroune showed the Vivero and Valdoviño fault zones to bound a crustal block that underwent internal deformation in relation to motion along the Valdoviño fault zone.

One of the main problems of the structure in NW Spain is the discrepancy between the NNE–SSW orientation of the stretching lineation in the crustal block bounded by Valdoviño and Vivero faults, and its NW orientation in the area around the Vivero fault. Due to its extensional character, the Vivero fault poses the problem of ascribing it to orogenic extension or only to local extension in an overall crustal shortening context. This study is focused on the analysis of the structures developed in an area straddling both sides of the Vivero fault zone in order to establish the deformational history there and develop a model for the regional tectonic evolution.

A detailed study of the nature of the relationships between structures generated during fault movement was undertaken in the best exposed area. Fault-related structures are compared with those in the hangingwall occurring as far west as the Ollo de Sapo anticline, and in the footwall in the westernmost part of the Mondoñedo nappe, in a belt extending from the coast southwards about 40 km to Roupar (Fig. 1).

The metamorphic evolution of the fault zone was also studied in order to explain the occurrence of kyanite in

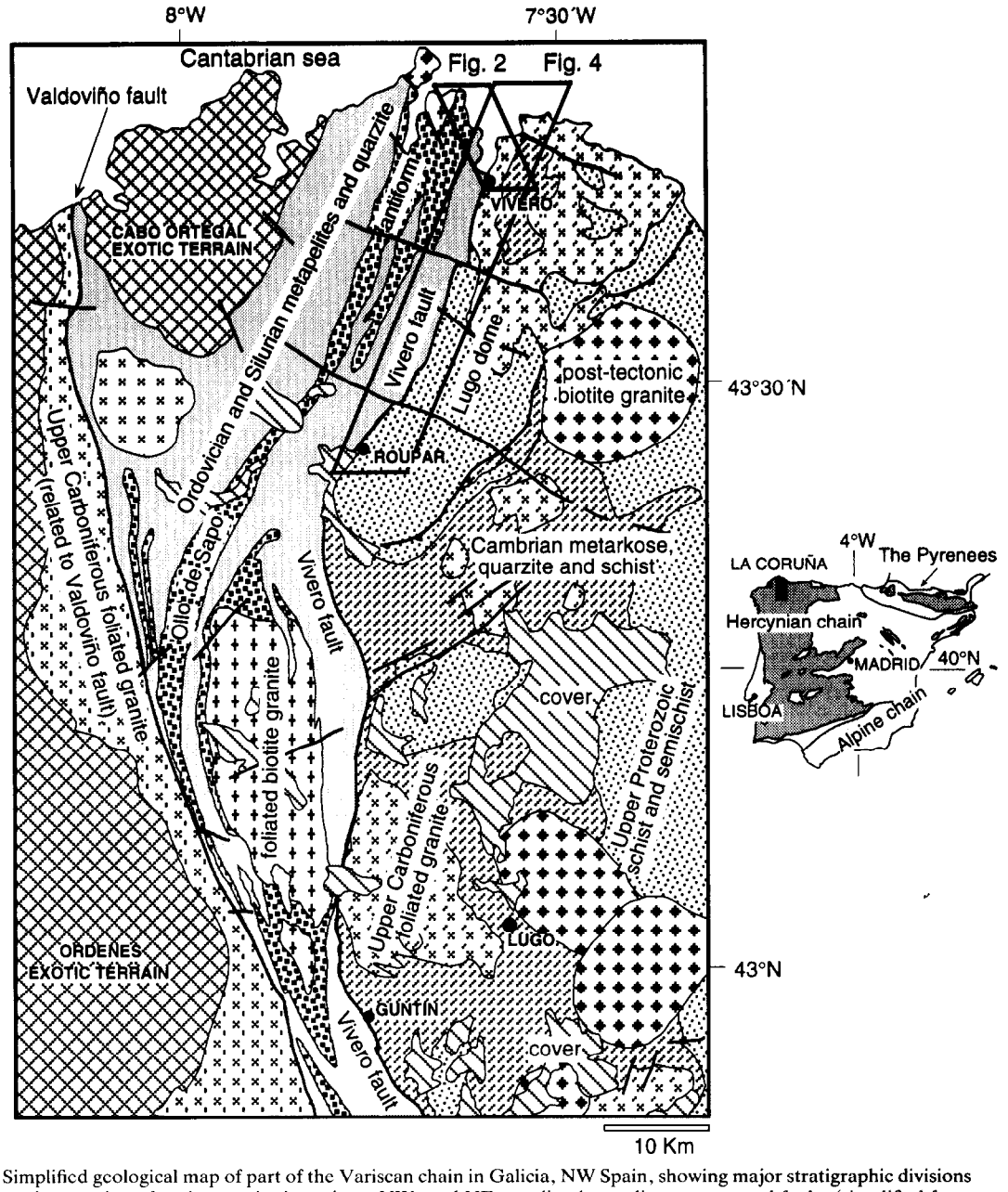

Fig. 1. Simplified geological map of part of the Variscan chain in Galicia, NW Spain, showing major stratigraphic divisions and tectonic grouping of major granite intrusions. NW- and NE-trending heavy lines are normal faults (simplified from Bastida *et al.* 1984, González-Lodeiro *et al.* 1982). Location of Figs. 2 and 4 is shown.

pelitic units with particular compositions, in bands parallel and close to the Vivero fault zone, and to deduce the *P–T* conditions under which the deformation related to the Vivero fault took place.

STRUCTURAL FRAMEWORK

The distribution of metamorphism in the internal part of Variscan chain in Spain is closely related to its structure (Martínez & Rôlet 1988). The higher grade areas are related to antiformal or domal structures in which abundant granitic plutons were intruded (Martínez *et al.* 1988). The Vivero fault is a N–S striking ductile shear zone separating two high grade metamorphic areas, the Lugo dome to the east, and an antiform cored by the Ollo de Sapo gneiss to the west. The fault extends from the Cantabrian coast near the town of Vivero to the south for 140 km (Fig. 1). The Lugo dome is a complex structure formed by refolding of the Mondoñedo nappe, an F_1 recumbent fold with a flat schistosity that was later thrust towards the east on a ductile shear zone (the Mondoñedo basal thrust of Bastida *et al.* 1986).

The Ollo de Sapo anticline (Parga-Pondal *et al.* 1964, Matte 1968, Ponce de León & Ribeiro 1981, González-Lodeiro 1983) is cored by the Ollo de Sapo gneiss composed of volcaniclastic, porphyritic quartzofeldspathic rocks of probable Cambrian age. The core of the anticline is bounded by Ordovician schist and quartzite. The overturned, eastern limb of the anticline belongs to a tight, upright F_2 syncline cored by rusty

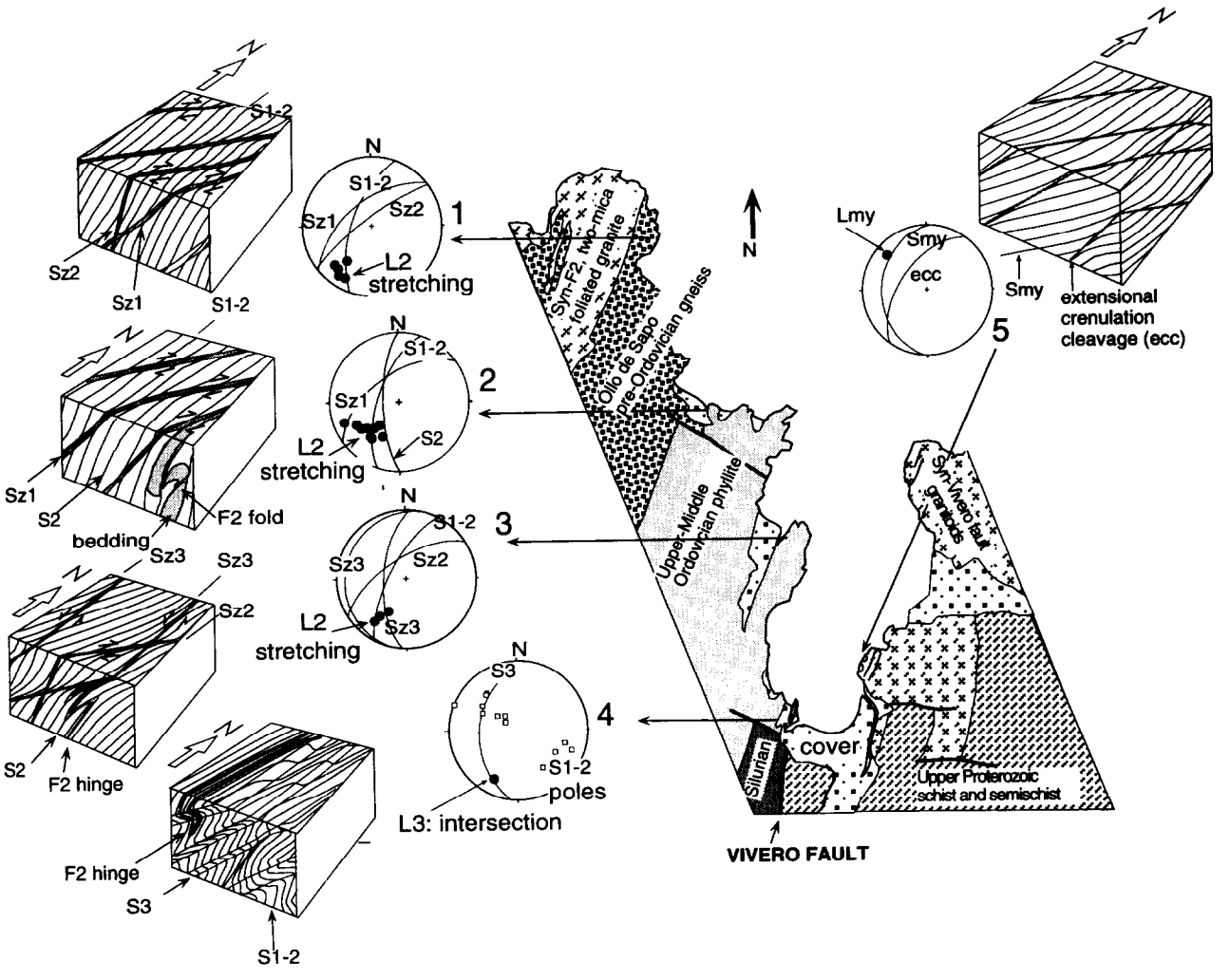

Fig. 2. Simplified geological map showing structural sites along the coastal section (detail of Fig. 1). At localities 1, 2, and 3, stretched and sheared F_2 folds deform bedding plus S_1. Block diagrams in outcrops 1–3 show Sz_1, Sz_2 and Sz_3 shear bands with different attitudes with respect to S_{1-2} as explained in the text. The block diagram at locality 4 shows F_3 kink-bands deforming F_2 folds and the composite S_{1-2} foliation. At locality 5, the Vivero fault mylonitic foliation, S_{my}, and the stretching lineation, L_{my}, are deformed by an extensional crenulation cleavage (ECC). All the stereoplots are lower hemisphere equal angle.

weathering, graphitic pelitic schist and minor quartzite, calc-silicate rock, and meta-limestone of Silurian age and truncated by the Vivero fault on its eastern limb.

The Vivero fault has long been recognized as an important boundary separating two different tectono-stratigraphic domains (Matte 1968, Capdevila 1969, Bastida *et al.* 1984, Martínez-Catalán 1985). Offset along the fault progressively decreases southwards to where the fault dies out into a syncline cored by Silurian black shales. The Vivero fault has been interpreted as a steeply dipping normal fault with downward movement of the western block (Matte 1968, Martínez-Catalán 1985, Bastida *et al.* 1986). Fault rocks in a broad zone within and along the fault zone are commonly mylonites.

Approaching the Lugo dome from the Ollo de Sapo antiform (Fig. 2), an S_1 axial planar foliation related to E verging F_1 structures is recognized. These F_1 structures are re-folded by asymmetric F_2 folds also E verging, with NNE trending, sub-horizontal axes and axial planes dipping consistently steeper than F_1 (González-Lodeiro 1983). Mesoscopic F_1 folds are almost coaxially re-folded by F_2 folds. Wherever they occur, F_2 folds contain a strongly developed, closely spaced crenulation cleavage, S_2, that almost completely transposes the earlier S_1. A sub-horizontal or gently SSW plunging, stretching lineation, L_2 (Rathore *et al.* 1983) is parallel to the F_2 fold axes.

An anastomosing network of three sets of shear bands with different local development (Sz_1, Sz_2 and Sz_3, at localities 1, 2 and 3 in Fig. 2) occur as a consequence of progressive deformation during F_2. These shear bands are less than 1 cm wide and, where well developed, form a penetrative fabric spaced about 2–5 cm apart. Viewed in sections approximately perpendicular to F_2 fold axes, two of the shear band sets (Sz_1 and Sz_3) dip more gently than the dominant foliation (Fig. 2) whereas the third set (Sz_2) is steeper. When seen in three dimensions, a dextral strike-slip movement with a minor reverse component is deduced for the sets of shear bands at localities 1 and 2 (Fig. 2).

This movement accommodated NNE–SSW stretching of F_2 folds evidenced by a shallowly plunging L_2 stretching lineation developed on the foliation within the shear bands and on quartz veins deformed by them. The L_2 is

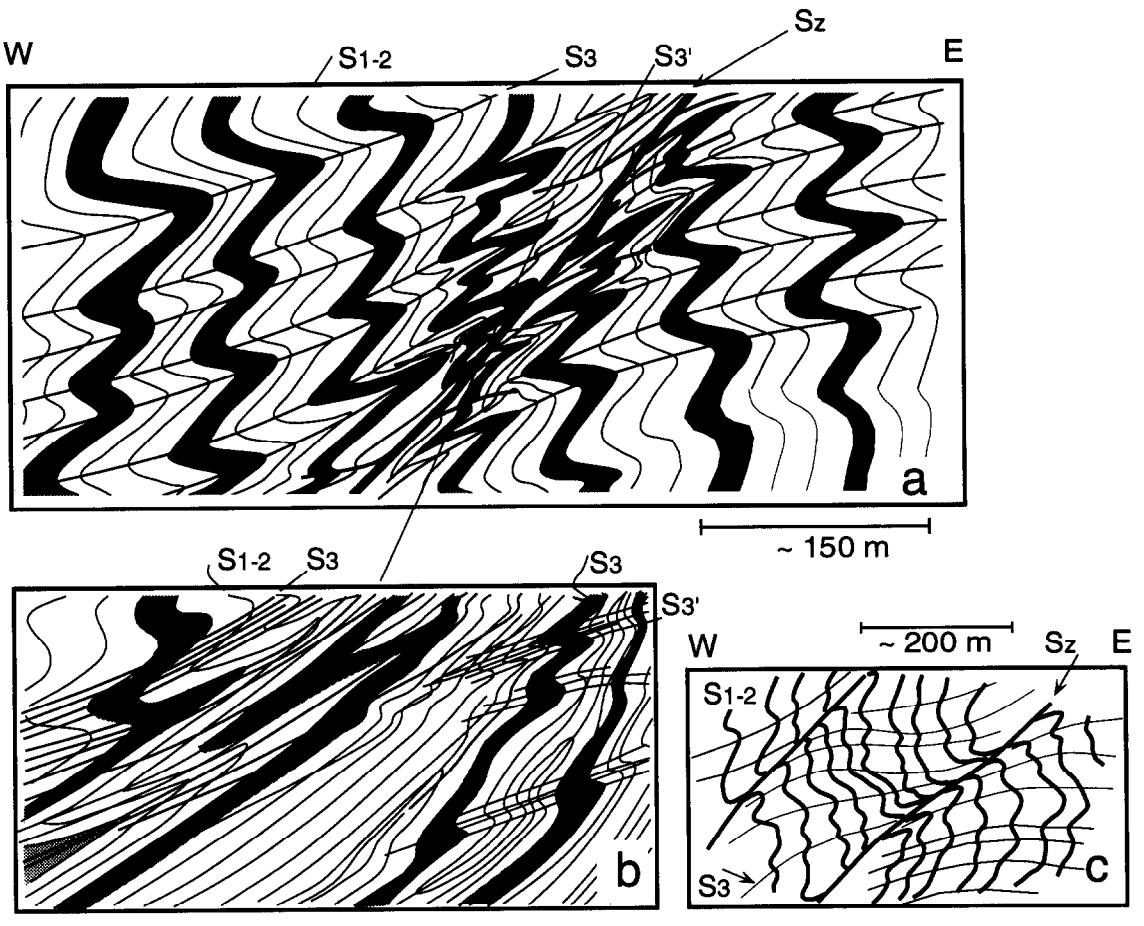

Fig. 3. (a) Detailed cross-section of the rusty Silurian schist near the Vivero fault, showing sub-horizontal F_3 folds deforming the composite regional foliation S_{1-2}. Crenulation cleavage, S_3, is deformed by minor normal shears responsible for local reversal of dip of S_3. (b) Closer view of the structures developed in high strain domains in the hangingwall adjacent to the Vivero fault zone, showing progressive re-folding and development of successive generations of sub-horizontal F_3 folds and S_3 crenulation cleavage. Sub-horizontal F_3 folds and their axial plane S_3 crenulation cleavage deform steeply dipping S_{1-2} (at left). More penetrative S_3 foliation is axial planar to isoclinal F_3 folds and, where most strongly developed, S_3 transposes S_{1-2} (right of centre). Steepening of S_3 near the fault leads to the development of new, sub-horizontal F_3 folds and a new axial plane cleavage, $S_{3'}$ (at right) that deform S_3. (c) Attitude of S_3 foliation in domains bounded by Vivero fault-like minor normal shears.

conspicuous where it is marked by pressure shadows on kyanite pseudomorphs of quiastolite porphyroblasts.

At locality 3 (Fig. 2), a northerly striking set of shear bands dipping variably and having a sinistral–normal movement was assigned to Sz_3; this set appears to have a reverse sense of movement in sections perpendicular to F_2 fold axes. The more easterly striking, sub-vertical set Sz_2 also present at localities 1 and 2 is related to a dextral-plus-minor reverse movement. In three dimensions (Fig. 2, locality 3), Sz_2 and Sz_3 make an angle of 60° and the dominant foliation plane bisects this angle. Thus, in horizontal sections, the shear bands appear as a conjugate dextral and sinistral set. The three dimensional arrangement of both sets at locality 3 is consistent with a bulk shortening perpendicular to the pre-existing S_{1-2} foliation.

THE VIVERO FAULT ZONE

Although the Vivero fault has been mapped as a line marking the boundary between the belt of Silurian pelite to the west and the Precambrian–Cambrian rocks of the margin of the Lugo dome to the east, there is, in fact, a broad zone where both groups of rocks have been deformed to variable degree. Granite intruded in the fault zone contains the same fault-related structures as those observed in the metasediments.

Deformation in the hangingwall

As the Vivero fault is approached from the west, new structures superimposed on the regional composite S_{1-2} foliation become prevalent. These superimposed structures have been examined in the fault zone from the coast southwards along strike for a distance of around 40 km to Roupar (Fig. 1). In the Silurian rocks of the hangingwall there is an approximately 2 km-wide zone in which the regional S_{1-2} is deformed by a well-developed system of F_3 folds with sub-horizontal axes (Figs. 2 and 3). The F_3 folds' axes trend predominantly NNE, subparallel to the fault zone but, due to non-cylindricity and the gentle dip of their axial planes, this trend is dispersed. They are open to tight asymmetric folds and

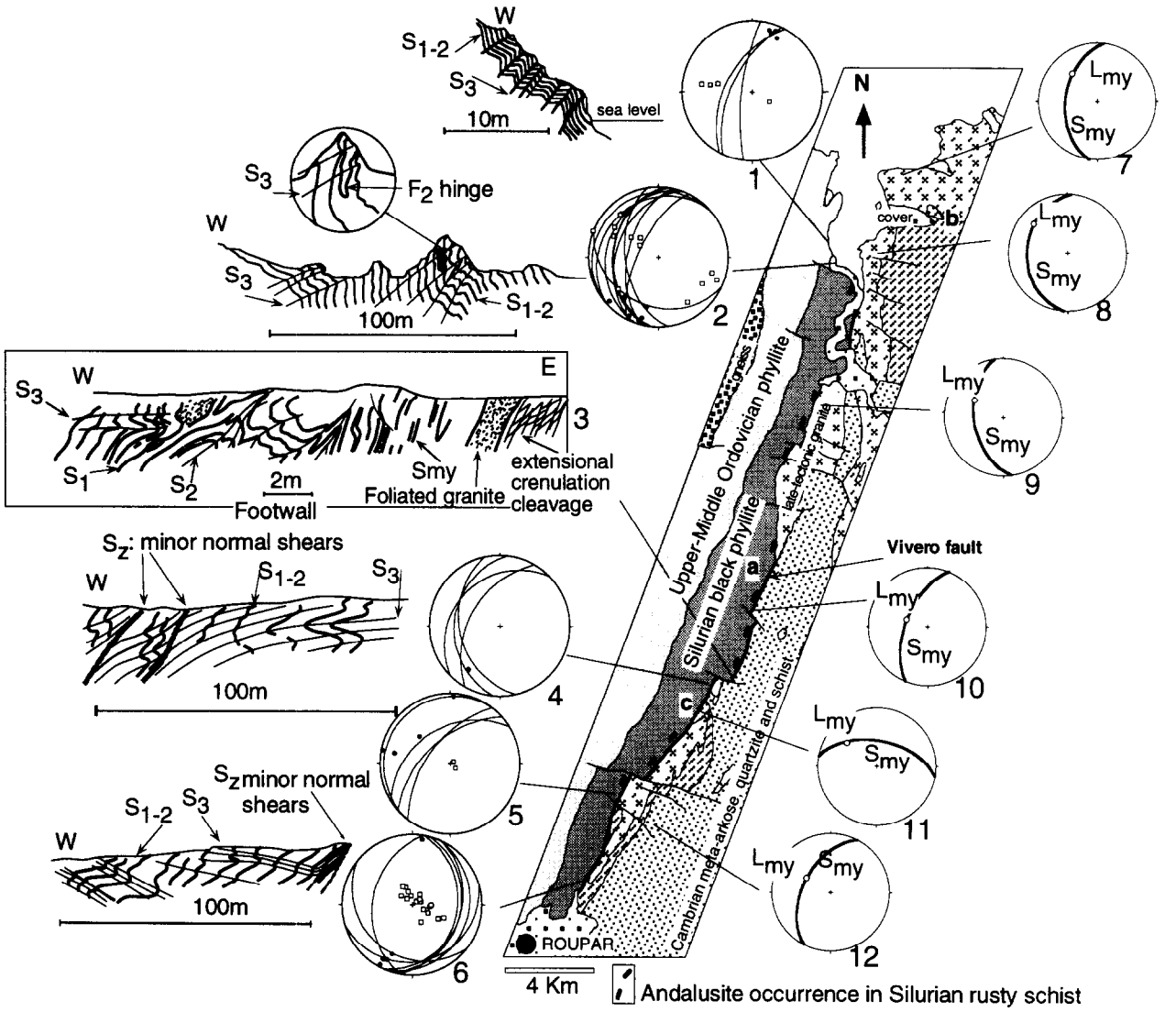

Fig. 4. Simplified geological map of the Vivero fault zone from the coast to Roupar. Also shown are the largest bodies of granite intruded along the fault zone; most are synkinematic with respect to fault movement, but one large granite in the fault zone is late tectonic. Cross-sections on left (numbers indicate localities) show sub-horizontal F_3 folds and their axial planar crenulation cleavage, S_3, deforming the regional S_1 and S_2 foliations. Steeply dipping lines, Sz, at localities 4 and 6 are minor normal shears with the same sense of slip as the Vivero fault. Equal angle stereoplots show sub-horizontal S_3 cleavage as planes, the axes of F_3 folds as dots, and poles to S_{1-2} as open squares. On the right-hand side is the orientation of mylonitic foliation, S_{my} (as planes) and mineral stretching lineation, L_{my} (as dots) in the fault zone. Mylonitic foliation is developed both in metasediments and in granite intrusions. See the text for discussion.

kink bands with wavelengths ranging from less than 10 cm to 10–20 m with an axial planar crenulation cleavage, S_3 (Fig. 3; locality 4 in Fig. 2; and localities 1–6 in Fig. 4).

Sets of sub-horizontal F_3 folds develop spatially related to steeply plunging minor normal shears Sz near the fault zone (Figs. 3a & c, and localities 4 and 6 in Fig. 4). Early formed, axial planar S_3 cleavage rotates as a consequence of progressive shearing and becomes deformed, causing the dispersion of F_3 axes (Fig. 3c). In higher strain domains, S_3 cleavage is steepened due to drag along Sz normal shears; S_3 then becomes re-folded by folds with sub-horizontal axial planes and a new crenulation cleavage $S_{3'}$ is developed as the result of a single progressive deformation event (for example, Figs. 3a & b; and localities 4 and 6 in Fig. 4).

Thus, F_3 folds grade from open-, kink-, or chevron-shaped folds with a weak S_3, in lower strain domains (localities 1 and 2 in Fig. 4) to tight, isoclinal folds with curved axes and a strongly developed, axial planar S_3 crenulation cleavage in higher strain domains. Higher strain domains become prevalent as the Vivero fault is approached (localities 4 and 5 in Fig. 4) and, in them, S_3 becomes a tectonic banding and the most penetrative foliation in outcrop, almost completely transposing S_{1-2}.

Locally, in less-deformed Silurian rocks, sub-vertical S_{1-2} foliation is deformed by two sets of kink-bands, the dominant set showing a top-to-the-west sense of movement and the other a top-to-the-east sense of movement (Fig. 5), implying the sub-vertical collapse of the pre-existing anisotropy. Granite veins are intruded along the axial surfaces of both sets of kink-bands (Fig. 6a).

Deformation in the footwall

Precambrian–Cambrian rocks of the Lugo dome adjacent to the Vivero fault contain a mylonitic fabric. In

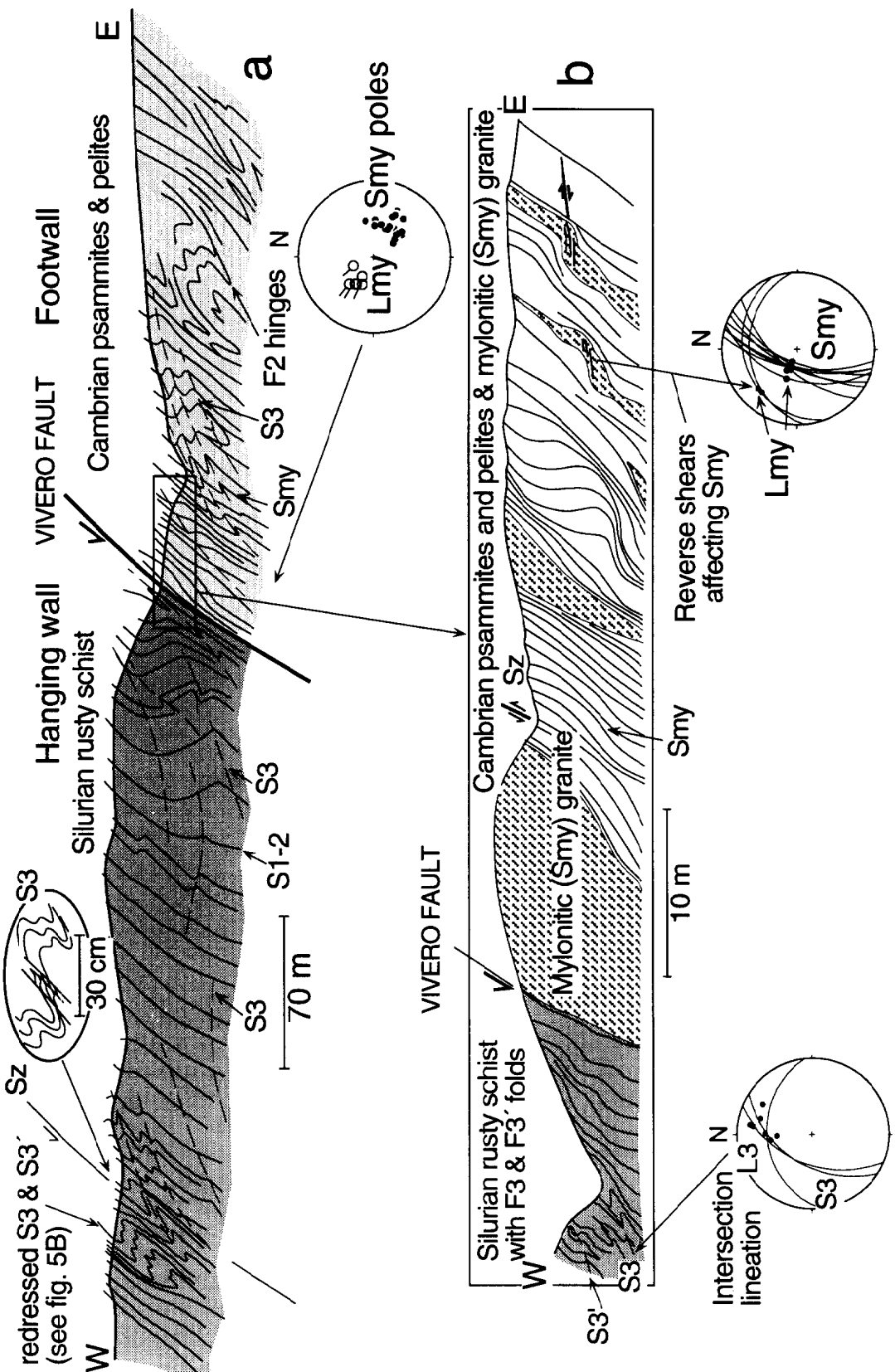

Fig. 5. Detailed cross-sections of the Vivero fault near locality A of Fig. 4. A high strain domain of concentrated slip in the hangingwall is shown on the upper section on the left-hand side; the gentle change in attitude of S_3 due to shearing produced by Sz shears is also shown. Lower detailed inset shows two conjugate shear sets. One of them (Sz) has the same sense of slip as the Vivero fault and the other has a reverse sense, antithetic to the normal Sz. Lower hemisphere equal angle stereoplots show the Vivero fault mylonitic foliation S_{my} deformed by both types of shears. Symbols: L_{my}, mylonitic lineation; L_3, intersection lineation.

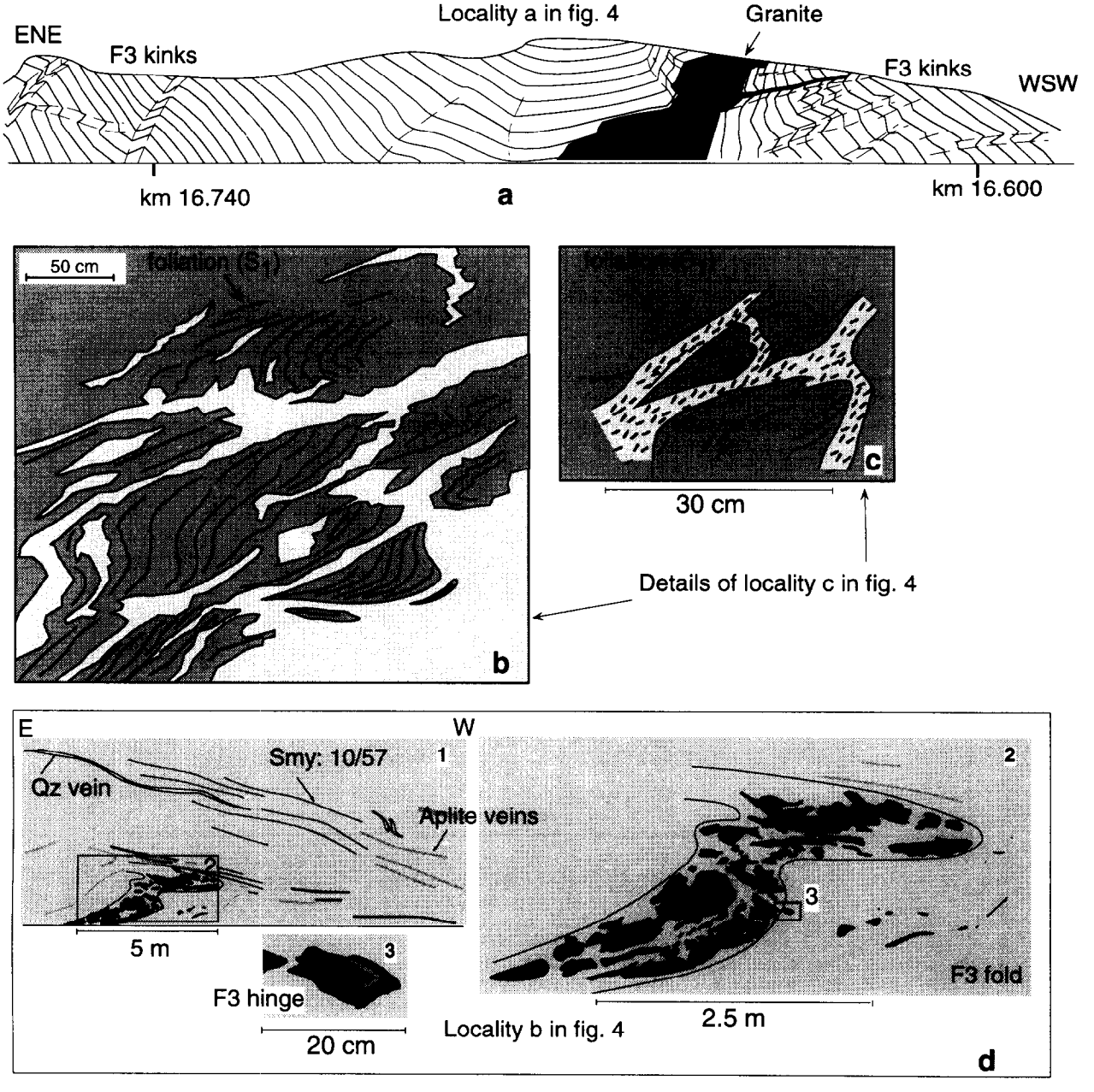

Fig. 6. Relations between successive generations of folds, mylonitic foliation, and granite in the fault zone and its vicinity. (a) Granite body intruded along conjugate kink bands in decametric F_3 fold in the rusty Silurian schist of the hangingwall. The sub-vertical kinks have a movement compatible with the Vivero fault whereas the sub-horizontal kinks, equivalent to S_3, are conjugate. (b) & (c) Small granite veins at locality c in Fig. 4. Veins occur in sets subparallel to the axial planes of F_2 folds and to their stretched limbs. (d) Numbers 1, 2 and 3 show a relic fold inside a granite deformed by the mylonitic foliation, S_{my}, at different scales. Aplite veins are also affected by S_{my} (at right). Psammitic rocks are dark grey, granite is grey.

strongly deformed domains, the mylonitic foliation, S_{my}, overprints bedding and re-worked S_{1-2} has an anastomosing appearance in metre-wide corridors (locality 3 in Figs. 4 and 5); S_{my} dips about 60°W with a strike parallel to the fault zone. A mineral stretching lineation, L_{my}, plunging steeply NW, and an extensional crenulation cleavage, dipping NW, widely developed in the fault zone permits deduction of a normal–dextral movement of the hangingwall (locality 5 in Fig. 2; localities 3 and 7–12 in Figs. 4 and 5). Similar attitudes for foliation and lineation in the Vivero fault zone have been described by Aranguren & Tubía (1992) some 60 km south of our studied area.

Strong deformation of sill-like granitic intrusions leads to the development of conspicuously layered rocks, composed of metre-thick layers of deformed granite alternating with phyllonitic metasediments in which remnant fold hinges are preserved. Mylonitized schist and phyllonite commonly have an oyster shell texture (Barker 1990, p. 100) produced by an anastomosing configuration of the extensional crenulation cleavage planes.

Remnants of F_2 hinges appear as 'fish-like' (Barker 1990, p. 101) rock bodies, tens of metres wide, bounded by sub-vertical shear zones with a normal fault movement (*Sz* in Fig. 5) similar to those found in the hanging-

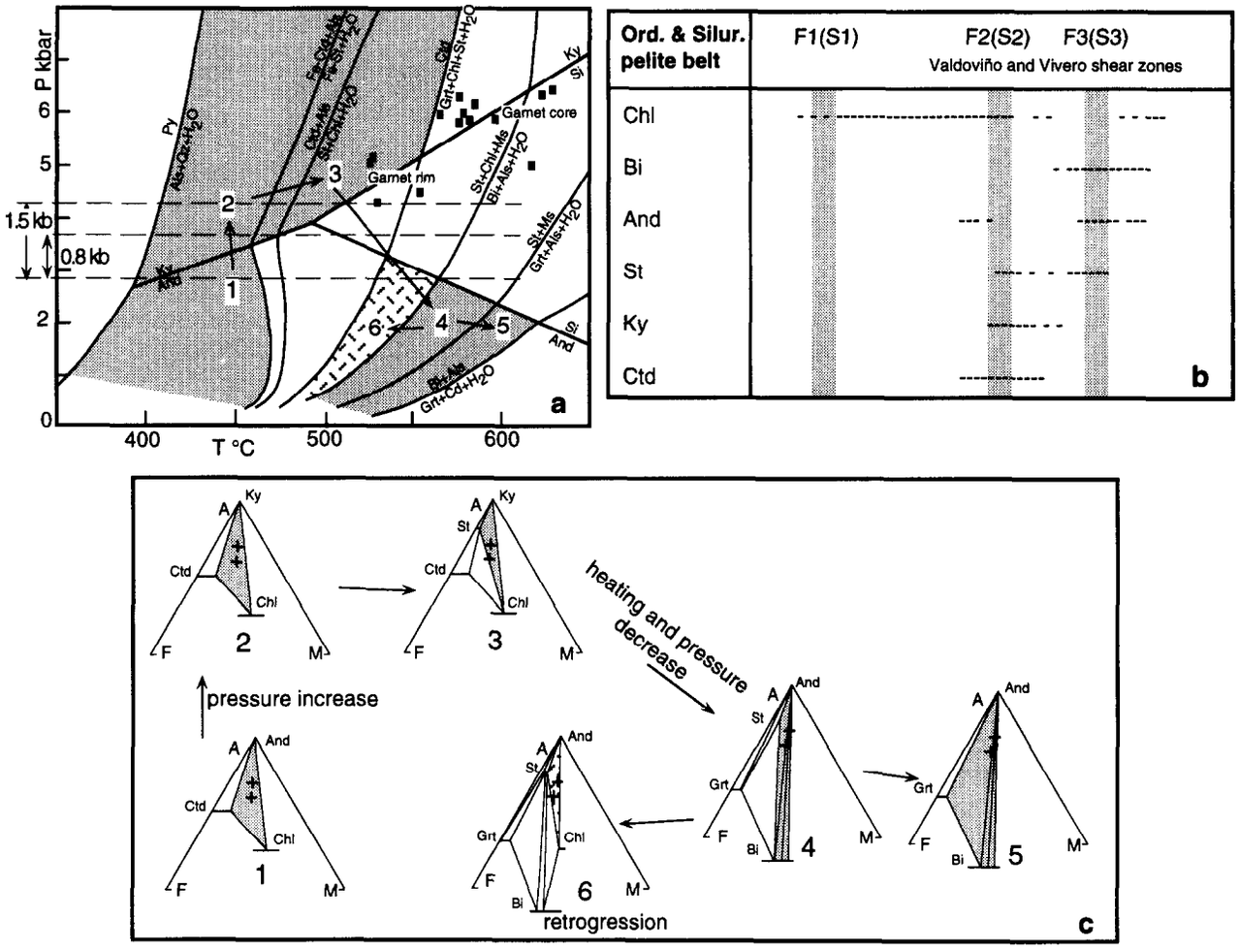

Fig. 7. (a) Paths for the Silurian–Ordovician hangingwall rocks west of the Vivero fault. Grey patterned fields bounded by reactions represent observed prograde assemblages. The assemblage 6 represents a retrograde chlorite-bearing assemblage in which biotite remains metastable. Black squares represent calculated *P–T* conditions for garnet cores and rims in footwall schist of the Lugo dome. Arrows on the *P*-axis indicate the minimum pressure difference between the footwall and hangingwall (1.5 kb) and between different parts of the Silurian rocks in the hangingwall (0.8 kb). See text for explanation. The KFMASH equilibria is after Spear & Cheney (1989). (b) Timing relations between deformational phases and crystal growth in the Vivero fault hangingwall. (c) AFM assemblages (after Spear 1993) recorded in black Ordovician and Silurian metapelite in the hangingwall of the Vivero fault. In assemblage 4, staurolite (st) plots inside the three-phase field grt-and-bi. Crosses represent Al-rich bulk composition as analysed by Briggs (1995). Symbols: bi = biotite, also = Al-silicate, and = andalusite, ky = kyanite, st = staurolite, ctd = chloritoid, chl = chlorite, ms = muscovite, q = quartz, grt = garnet, cd = cordierite, qz = quartz.

wall. The F_2 folds are locally re-folded by sub-horizontal F_3 folds similar to those in the Silurian schist of the hangingwall (locality 4 in Fig. 4). Mylonitic granite veins containing a W plunging stretching lineation, L_{my}, are deformed by reverse shears antithetic to the sub-vertical *Sz* (Fig. 5). Granite is intruded along both shear sets (Figs. 6b & c) and continuous shearing during intrusion caused granite mylonitization.

METAMORPHIC EVOLUTION

Mineral assemblages

A series of mineral assemblages are observed in the belt of Ordovician and Silurian pelite situated between the Ollo de Sapo gneiss and the Vivero fault. Assemblages with kyanite, chloritoid, and staurolite (2 and 3 in Figs. 7a & c) appear restricted to very Al-rich compositions in graphitic metapelite in the hangingwall. The following description refers to these compositions.

The common assemblages in the graphitic metapelite contain chloritoid–muscovite ± chlorite and chloritoid–muscovite–kyanite ± chlorite (2 in Fig. 7c), both without biotite. These assemblages develop synkinematically with the S_2 sub-vertical crenulation cleavage (Fig. 7b) and occur throughout black Ordovician and Silurian slate and phyllite up to the western margin of the Vivero fault zone where the later S_3 sub-horizontal tectonic banding first appears. Locally, syn-S_2 and mainly syn-S_3 staurolite rims kyanite, defining the higher-temperature assemblage muscovite–kyanite–chlorite–staurolite, in which chloritoid still remains in the matrix (3 in

Figs. 7a & c). In assemblage 2, kyanite occurs in the rock matrix and as kyanite–muscovite aggregates pseudomorphing pre-existing, sub-idiomorphic chiastolite. Relics of chiastolite occur locally in this zone of slate and phyllite. Pseudomorphed quiastolite is pre-S_2 and its existence implies early conditions given by assemblage andalusite–chloritoid–muscovite (1 in Fig. 7a) at pressure below the andalusite–kyanite phase boundary, although quiastolite and chloritoid have not yet been found in contact.

Passage from the assemblage 1 to assemblages 2 or 3 with stable kyanite represents a significant increase in pressure that would take the rocks far enough into the kyanite field to allow kyanite to be nucleated on andalusite through ionic reactions involving K^+ and H^+, producing intermediate muscovite (Carmichael 1969). The local presence of assemblage 3 (Fig. 7c), containing muscovite–kyanite–chlorite–staurolite, suggests that conditions during F_2 folding and initial movement along the Vivero fault were near those required for assemblage 3 (Fig. 7a) in the kyanite stability field.

Chloritoid is abundant where kyanite occurs and it is stable in Al-rich compositions in the hangingwall to within 100 m of the fault, where Silurian rocks are in contact with rocks of the Lugo dome. In addition, decimetric veins composed of quartz–kyanite ± muscovite occur in the Silurian phyllites and are commonly folded by sub-horizontal F_3 folds. Within this 100 m-wide zone adjacent to the fault contact, the chlorite-free assemblage staurolite–biotite–muscovite–andalusite (4 in Figs 7a & c) is found in the same Al-rich rocks. These occurrences imply that temperature conditions below the upper limit of chloritoid + kyanite stability mostly prevailed in the hangingwall, except in local places with the assemblage 3 and within a narrow zone adjacent to the fault contact between hangingwall and footwall rocks.

This 100 m-wide strip of Silurian rocks adjacent to the fault contains massive, dense, black, hornfels-like schist with conspicuous rusty weathering that is the product of contact metamorphism (Fig. 4). This Silurian rusty schist is not continuous along strike but seems to form layers alternating with Al-poorer semi-schist and psammite that contain the assemblage garnet–biotite–chlorite–muscovite.

The stable assemblage in the rusty Silurian schist is staurolite–andalusite–biotite–muscovite (4 in Fig. 7c), and locally, the higher T assemblage andalusite–garnet–biotite–muscovite is present (5 in Figs. 7a & b). In the rusty schist, quartz–andalusite veins accompany the quartz–kyanite ± muscovite veins found elsewhere to the west in the hangingwall.

Pleochroic, porphyroblastic andalusite, instead of kyanite, is abundant in assemblage 4, and occurs syn- to post-S_3 (Fig. 7b). In assemblage 4, staurolite is synchronous with the development of the sub-horizontal S_3 cleavage, is abundant in the matrix, and also occurs partially resorbed inside andalusite–biotite aggregates and in blastic plagioclase. Staurolite and biotite are stable in the rusty schist always in the presence of andalusite, never with kyanite. Relics of kyanite only occur as inclusions in porphyroblastic plagioclase and less often in andalusite.

These mineral relations mean that the rusty Silurian schist developed during progressive increase in temperature inside field 4 (Figs. 7a & c) causing the progressive consumption of staurolite through the continuous KFMASH, porphyroblastic andalusite-forming reaction: muscovite + staurolite + quartz = andalusite + biotite + H_2O. The rusty schist continued eventually along a prograde path crossing the univariant staurolite-out reaction shown in Fig. 7a and reaching conditions given by assemblage 5 (Figs. 7a & c). The passage from the assemblage 3 with kyanite, to the higher T assemblage 4 with andalusite, records pressure decrease and heating (Fig. 7a) which are interpreted as due to uplift of the hangingwall and heat transferred into it from the hotter footwall and from granites intruded into the fault zone. Therefore, in the hangingwall, there is a narrow, discontinuous strip of rocks that have been uplifted and contain lower P, higher T mineral assemblages than the rest of the rocks further west. We interpret the metamorphic evidence to show that deformation inside the Vivero fault zone was concentrated in more than one shear zone, and the contact between the andalusite-bearing Silurian schist and the kyanite-bearing, lower grade Silurian to the west is a concentrated slip zone situated west of the main Vivero fault affecting Silurian rocks.

A small amount of chlorite occurs with staurolite–andalusite–biotite–muscovite (assemblage 4) forming the apparently metastable, four-phase, univariant assemblage 6 (Figs. 7a & c) which requires a decrease in T to reverse the reaction chlorite + muscovite + staurolite = biotite + aluminum silicate + quartz + H_2O (Fig. 7a). Biotite should be unstable in assemblage 6 for the Al-rich bulk rock compositions considered. Retrograde chlorite locally records the latest Vivero fault movements occurring in discrete Sz surfaces with normal fault movement in Silurian rocks, in extensional crenulation cleavage in the Precambrian–Cambrian (Figs. 2, 3 and 5), and also as a post-kinematic mineral.

Pressure–temperature conditions in the footwall have been calculated on the basis of the assemblage plagioclase–garnet–biotite–quartz–muscovite found in semi-pelite of the Lugo dome, close to the Vivero fault (Table 1). Applying garnet–matrix biotite thermometry (Hodges & Spear 1982) together with garnet–biotite–muscovite–plagioclase barometry (Ghent & Stout 1981, Fig. 7a) conditions of 6.4–5.8 kb and 620–570°C have been obtained for garnet cores. Conditions deduced from the rim of partially resorbed garnets are 4.3–5.1 kb and 530–550°C (Fig. 7a). These garnets are S_i-free but are wrapped by the composite S_{1-2} fabric in the footwall.

Geologic implications of the metamorphism

Maximum pressure conditions estimated for assemblage 4 in the hangingwall are around 2.8 kb, and minimum pressure estimated for garnet rims in the

Table 1. Electron microprobe mineral analyses in footwall schist of the Lugo dome adjacent to the Vivero fault

Garnet	Core	Core	Core	Core	Core	Core	Core	Core	Core	Core	Rim	Rim	Rim	Rim	Matrix plagioclase		Matrix micas	Biotite	Muscovite
SiO_2	37.14	37.37	37.56	37.48	37.37	37.44	37.24	37.77	37.82	37.66	37.47	37.29	37.01	37.61	SiO_2	61.58	SiO_2	35.33	46.72
TiO_2	0.04	0.04	0.05	0	0.04	0.04	0.05	0	0.02	0.01	0	0.02	0	0.02	Al_2O_3	25.42	TiO_2	1.5	0.52
Al_2O_3	21.22	21.86	21.73	21.49	21.76	22.04	21.93	21.68	21.73	21.48	21.52	21.16	21.4	21.8	Fe_2O_3	0.07	Al_2O_3	19.72	38.81
Cr_2O_3	0	0	0.06	0	0.02	0.01	0.04	0.04	0	0.05	0.09	0	0.01	0	CaO	6.04	Cr_2O_3	0.1	0.06
FeO	33.1	32.65	32.3	32.66	31.86	32.54	32.86	33.96	31.87	32.22	33.7	33.51	34.12	34.78	Na_2O	8.28	FeO	17.65	1.08
MnO	3.03	3.2	3.36	3.19	3.37	3.37	3.16	2.94	3.14	3.34	3.27	3.39	2.57	2.95	K_2O	0.06	MnO	0.15	0
MgO	3.45	3.4	3.45	3.49	3.27	3.26	3.7	4.17	3.83	3.87	3.03	3.06	3.49	3.33	Total	101.45	MgO	11.82	0.7
CaO	3.45	3.66	3.77	3.44	4.19	3.8	3.29	2.24	3.75	3.66	3.04	2.88	2.13	2.09			Na_2O	0.12	1.03
Total	101.44	102.17	102.29	101.75	101.87	102.49	102.27	102.81	102.16	102.29	102.13	101.3	100.73	102.57	Cations		K_2O	9.45	9.42
															Si	2.7	H_2O	4	4.55
Cations															Al	1.31	Total	99.86	102.89
Si IV	2.29	2.94	2.95	2.96	2.95	2.94	2.93	2.95	2.96	2.96	2.96	2.97	2.96	2.96	Fe^{+3}	0			
Al IV	0.05	0.06	0.05	0.04	0.05	0.06	0.07	0.05	0.04	0.04	0.04	0.03	0.04	0.04	Ca	0.28	Cations		
T site	3	3	3	3	3	3	3	3	3	3	3	3	3	3	Na	0.7	Si IV	5.3	5.98
															K	0	Al IV	2.7	2.02
Al VI	1.94	1.97	1.96	1.96	1.97	1.98	1.96	1.95	1.97	1.94	1.97	1.96	1.98	1.98			Ti IV	0	0
Cr	0	0	0	0	0	0	0	0	0	0	0.01	0	0	0	End members		T site	8	8
O site	1.94	1.97	1.97	1.96	1.97	1.98	1.97	1.96	1.97	1.95	1.97	1.96	1.98	1.98	AB	0,714			
															AN	0,286	Al VI	0.79	3.84
Fe^{+2}	2.2	2.15	2.12	2.16	2.1	2.14	2.16	2.22	2.09	2.12	2.23	2.23	2.28	2.29	KFS	0	Ti VI	0.17	0.05
Mn^{+2}	0.2	0.21	0.22	0.21	0.22	0.22	0.21	0.19	0.21	0.22	0.22	0.23	0.17	0.2			Cr	0.01	0.01
Mg	0.41	0.4	0.4	0.41	0.38	0.38	0.43	0.49	0.45	0.45	0.36	0.36	0.42	0.39			Fe^{+2}	2.22	0.12
Ca	0.29	0.31	0.32	0.29	0.35	0.32	0.28	0.19	0.31	0.31	0.26	0.25	0.18	0.18			Mn^{+2}	0.02	0
A site	3.11	3.07	3.07	3.07	3.06	3.06	3.08	3.09	3.06	3.1	3.06	3.07	3.05	3.05			Mg	2.65	0.13
O	12	12	12	12	12	12	12	12	12	12	12	12	12	12			O site	5.85	4.14
Al	0.71	0.7	0.69	0.7	0.69	0.7	0.7	0.72	0.68	0.68	0.73	0.73	0.75	0.75					
Py	0.13	0.13	0.13	0.13	0.12	0.12	0.14	0.16	0.15	0.15	0.12	0.12	0.14	0.13					
Sp	0.06	0.07	0.07	0.07	0.07	0.07	0.07	0.06	0.07	0.07	0.07	0.07	0.06	0.07					
Gr	0.09	0.1	0.01	0.09	0.11	0.1	0.09	0.06	0.1	0.1	0.08	0.08	0.06	0.06					

footwall is 4.3 kb (Fig. 7a). A pressure difference of about 1.5 kb results for rocks situated on opposite sides of the Vivero fault at the present erosional surface. Assuming a density of 2.75 g cm^{-3} (Olhoeft & Johnson 1989), a minimum throw of 5.5 km can be deduced for the fault.

Granite sills in the Ollo de Sapo gneiss deformed by F_2 folds (for example, the foliated, two-mica granite in the northwest in Figs. 2 and 9) appear to be responsible for the pre-S_2 quiastolite which was transformed into kyanite in the black Ordovician and Silurian metapelite of the hangingwall. Throughout most of the hangingwall, assemblages 2 (chloritoid–muscovite–kyanite ± chlorite) and 3 (muscovite–kyanite–chlorite–staurolite) remained undisturbed by the later low P, high T metamorphism recorded in the Vivero fault zone. This low P thermal event is restricted to the vicinity of the fault where contact metamorphism was induced by heat supplied to the hangingwall by the hotter rocks of the Lugo dome and by abundant veins of non-homogeneous biotite granite intruded along the fault zone (Fig. 4).

This contact metamorphism along the Vivero fault is synchronous with fault slip: assemblages 4 and 5 (andalusite ± garnet–biotite–muscovite–staurolite) are syn- to post-S_3, the crenulation of the fault-related F_3 folds. In Silurian pelite, the mylonitic fabric of the Vivero fault is defined by biotite and muscovite wrapping around andalusite and staurolite (± garnet). Biotite and muscovite are also stable in fault mylonites developed in the Precambrian–Cambrian of the Lugo dome and in mylonitic granites along the fault zone.

Prior to F_2 folding, hangingwall rocks were stable in the andalusite field at shallow depth. The pressure increase recorded by assemblages 1 and 2, with kyanite overgrowing earlier quiastolite, is evidence for rocks being down-dragged due to infolding into an F_2 synform. The fact that pre-F_2 quiastolite is replaced by kyanite in favourable hangingwall lithologies, synkinematically with the development of S_2 sub-vertical crenulation cleavage, indicates that downward movement took place during F_2 folding.

The occurrence of syn-F_2 and syn-F_3 staurolite in the hangingwall where it locally rims kyanite and makes part of assemblage 3 strongly suggests that the development of F_2 and F_3 folding was continuous in time. The F_3 folding started under conditions in the kyanite field and continued during uplift.

Decompression between stages 3 and 4 in the rusty Silurian schist (Fig. 7) implies that earlier kyanite-bearing pelite of the hangingwall, formed before faulting, was tectonically uplifted at least ~2.9 km (~0.8 kb; see Fig. 7a), accreted to the western side of the Lugo dome, and heated. Deformation inside the Vivero fault zone could have been partitioned into zones of concentrated slip. This would explain how the rusty Silurian schist of the hangingwall in contact with the Lugo dome was first dragged down by F_2 folding and then uplifted, attached to the footwall, during later movement on a secondary shear zone (Fig. 5a) situated to west of the main fault.

GRANITE INTRUSIONS IN THE VIVERO FAULT ZONE AND ADJACENT AREAS

In the northern sector of the Vivero fault zone, for a distance of about 30 km, the contact between Silurian schist and Precambrian–Cambrian quartzo-feldspathic granofels and gneiss is marked in places by mappable, sill-like granite intrusions of variable width (Figs. 1 and 4). In the Silurian rusty schist, small granitic bodies are found intruded along conjugate F_3 kink bands (Fig. 6a).

Similar, but smaller intrusions of granite are present all along the Vivero fault zone (Fig. 4), although they are more abundant in the quartzo-feldspathic rocks in the footwall. Intrusions occur either along Sz normal shears or along reverse shears antithetic to them (Figs. 6b & c). These intrusive relations are present for 2–3 km eastwards into the Lugo dome where granitic bodies occupy most of the outcrop, and hence their relations with their host rocks cannot be observed.

The intrusion of granite appears to be synchronous with slip on the Vivero fault as evidenced by the fact that granite contains xenoliths of folded Silurian schist and is itself deformed by the heterogeneously developed S_{my} mylonitic foliation (Fig. 6d). Similar relations were found farther south by Aranguren & Tubía (1992).

The intrusion of late- and post-tectonic granite (Fig. 4) sealed the fault movement and produced an undeformed contact metamorphism in the Silurian rocks along the fault zone.

REGIONAL TECTONIC SIGNIFICANCE OF THE VIVERO FAULT

The Lugo dome and the Ollo de Sapo antiform have long been considered to be F_2 folds (Matte 1968). Regional scale F_2 structures in the studied area are thus the Ollo de Sapo antiform and the syncline cored by Silurian pelite west of the Vivero fault. Although similar large-scale F_2 folds are not visible east of the Vivero fault, outcrop scale folds with axial planar S_2 are common in the footwall where they appear surrounded by mylonitic foliation related to the Vivero fault zone (see Figs. 4a and 9).

West of the Vivero fault zone, the Valdoviño fault, a steep, sinistral shear zone (Fig. 1), has been shown to be contemporaneous with F_2 folding (Ponce de León & Choukroune 1980). Ponce de León and Choukroune related minor conjugate dextral shear zones and subhorizontal F_2 fold axes, oriented parallel to a N–S stretching lineation L_2, to deformation by shearing. In our study area, the conjugate shear bands Sz_1 and Sz_2 and the stretching lineation L_2 on the east side of the Ollo de Sapo antiform (localities 1–3 in Fig. 2) also account for NNE–SSW progressive stretching inside the crustal block bounded by the Valdoviño and Vivero faults. The existence of F_2 folds and conjugate sets of shear bands related to them in the Ollo de Sapo antiform in the hangingwall of the Vivero fault indicate simul-

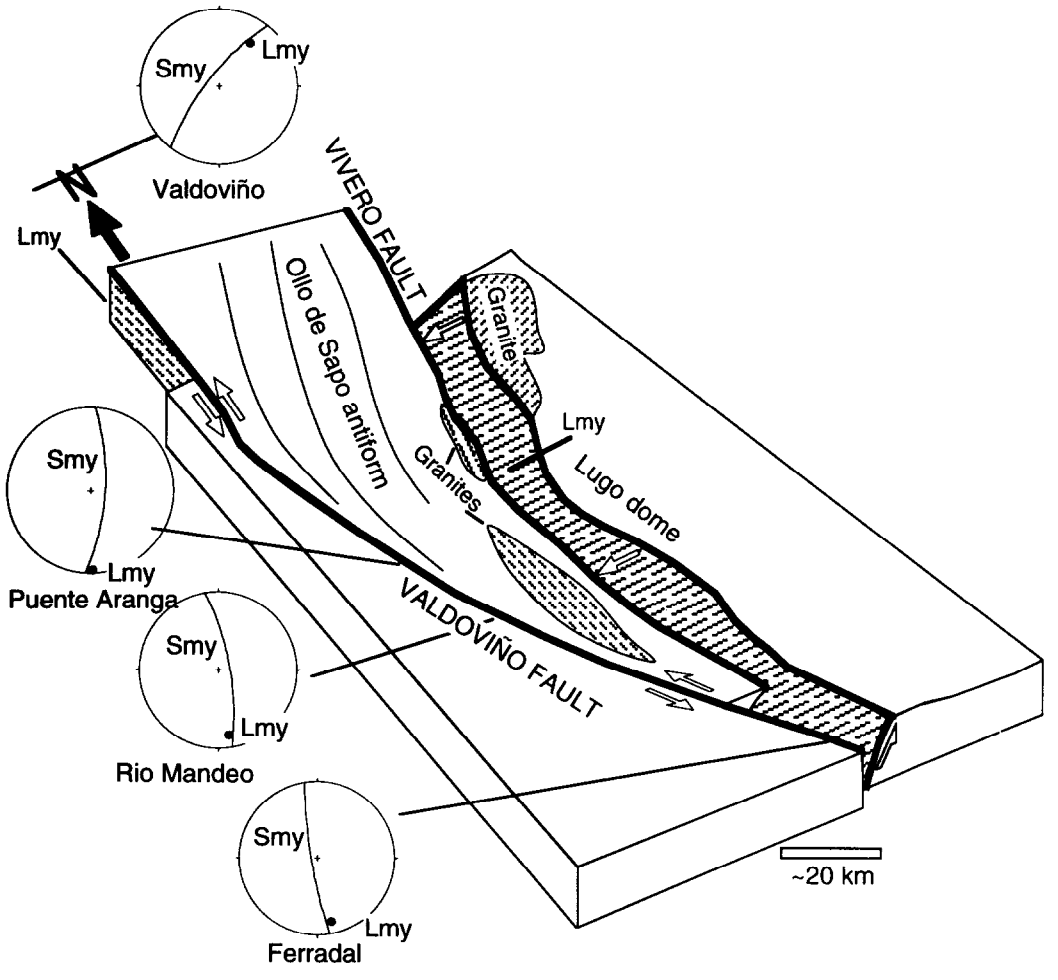

Fig. 8. Block diagram showing the overall pattern of movement within the crustal block bounded by the Valdoviño and Vivero faults. Both faults are mylonitic zones with a mineral stretching lineation, L_{my}, in mylonitic schistosity, S_{my}. The overall pattern of movement within the block is compatible with a bulk E–W crustal shortening. Stereoplots are lower-hemisphere equal angle.

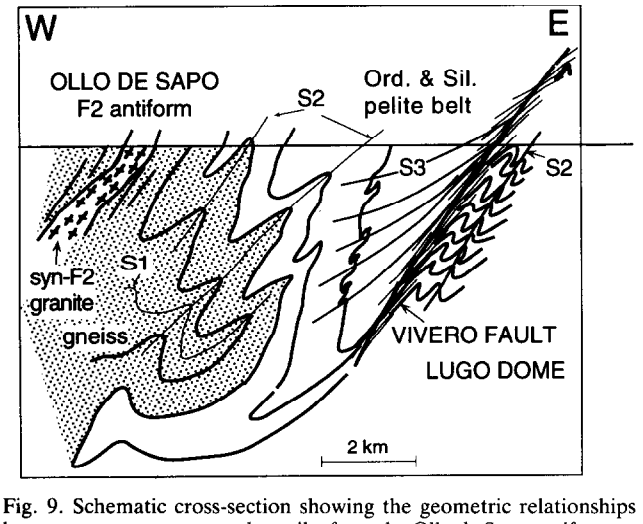

Fig. 9. Schematic cross-section showing the geometric relationships between structures across the strike from the Ollo de Sapo antiform to the western limb of the Lugo dome.

taneous E–W shortening and N–S stretching, suggesting a transpressive deformation regime for the area.

Strike-slip movement on the Valdoviño fault induced local extension to the east that was accommodated by development of the Vivero fault (Fig. 8). This fault was nucleated during the later stages of F_2 folding, once the Valdoviño fault began to move. At the initiation of Valdoviño fault movement, the eastern limb of the Ordovician–Silurian syncline must have been the most favourably oriented area to extend by shearing under the local stress field. Once nucleated, cumulative slip on the Vivero fault increased coevally with that on the Valdoviño fault. Compatibility of both fault movements is justified when balancing the E–W shortening and extension induced, respectively, by the Valdoviño sinistral strike-slip fault and the Vivero oblique-slip normal fault. Based on geometric grounds, a minimum likely displacement of 25 km on the Valdoviño fault produces 8 km of E–W crustal shortening, while the E–W extension produced by a 5.5 km throw on the Vivero fault does not exceed 3 km. This suggests that the northwards lateral escape of the Vivero–Valdoviño fault-bounded block during a bulk E–W directed crustal shortening is compatible with the local development of a local transtensional regime along the Vivero fault zone. The widespread syntectonic emplacement of granitoids along and adjacent to the Vivero fault zone was favoured in this transtensional regime.

CONCLUSIONS

The Vivero fault is a ductile normal shear zone developed in a local transtensional environment within a larger-scale, transpressive regime causing crustal shortening. The fault was generated during the process of E–W shortening of the Variscan chain which produced steep, E-verging F_2 folding. The fault was nucleated during the later stages of F_2 folding on the eastern limb of an F_2 synform situated between the Ollo de Sapo antiform and the Lugo dome, and is kinematically related to the sinistral movement of the transcurrent Valdoviño shear zone (Figs. 8 & 9). Coeval slip on the Valdoviño and Vivero faults forced the crustal block bounded by these faults to escape northwards, causing stretching of F_2 folds parallel to L_2 stretching lineation and extension on the Vivero fault.

Shearing related to the Vivero fault produced a W-dipping mylonitic foliation on which a NW-plunging stretching lineation indicates normal slip. In the vicinity of the fault, sub-horizontal F_3 folds with an axial planar S_3 cleavage deform the earlier-formed, composite sub-vertical S_{1-2} fabric.

Mineral assemblages in the hangingwall yield a maximum pressure of 2.8 Kb, whereas footwall rocks in contact with them give a minimum pressure of 4.3 Kb, allowing a minimum throw of 5.5 km for the Vivero fault.

Prior to F_2 folding, the hangingwall rocks were located at relatively shallow crustal levels in the andalusite stability field at conditions around 450°C and below 3.5 Kb. During F_2 folding, these rocks were sunk in a synform deep enough to produce the andalusite–kyanite transformation at conditions above 3.5 Kb and 450–500°C. During F_3 folding, local contact metamorphism at less than 2.8 Kb for temperatures approximately 600°C was induced in Silurian pelite of the hangingwall close to the fault contact with rocks of the Lugo dome.

Small granitic bodies were intruded along conjugate sets of F_3 folds in the hangingwall and in conjugate sets of shear bands in the footwall. Intrusion of younger, post-kinematic granite seals the fault and produce a static contact metamorphism.

Acknowledgements—We thank M. Julivert and A. Teixell for their helpful review of the manuscript. Also, thanks are given to M. Atherton for his kind review of the section about metamorphism. Fieldwork and travel for this research was made possible by DGICYT Research Project PB-91-0490 (to M.L.A.); NATO International Scientific Exchange Programmes Collaborative Research Grant 890371 (to C.D. and F.J.M.) and the Bucher Travel Fund of the Department of Geology, University of Cincinnati (to C.D.). We gratefully acknowledge all of these sources of support. Gracious hospitality to F.J.M. was provided by E. Ward. Gracious hospitality to C.D. was provided by M. L. Arboleya.

REFERENCES

Aranguren, A. & Tubía, J. M. 1992. Structural evidence for the relationship between thrusts, extensional faults and granite intrusions in the Variscan belt of Galicia (Spain). *J. Struct. Geol.* **14**, 1229–1237.

Barker, A. J. 1990. *Introduction to Metamorphic Textures and Microstructures*. Blackie, London.

Bastida, F., Marcos, A., Marquínez, J., Martínez-Catalán, J. R., Pérez-Estaún, A. & Pulgar, J. A. 1984. Geological Map of Spain S: 1:200,000, Sheet No 1: La Coruña. *Instituto Geológico y Minero de España*, Madrid, Spain.

Bastida, F., Martínez-Catalán, J. R. & Pulgar, J. A. 1986. Structural, metamorphic and magmatic history of the Mondoñedo nappe (Hercynian belt, NW Spain). *J. Struct. Geol.* **8**, 415–430.

Berthé, D. & Brun, J. P. 1980. Evolution of folds during progressive shear in the South Armorican shear zone. *J. Struct. Geol.* **2**, 127–133.

Berthé, D., Choukroune, P. & Jegouzo, P. 1979. Orthogneiss, mylonite and non-coaxial deformation of granites: the example of the South Armorican Shear Zone. *J. Struct. Geol.* **1**, 31–42.

Briggs, W. D. 1995. Pressure–temperature deformation history of the Ollo de Sapo antiform, Variscan orogen, northwest Spain. Unpublished Ph.D. dissertation, University of Cincinnati.

Capdevila, R. 1969. Le métamorphisme régional progressif et les granites dans le segment hercynien de Galice nord oriental (NW de l'Espagne). Unpublished Ph.D. thesis, Université de Montpellier, France.

Carmichael, D. M. 1969. On the mechanism of prograde metamorphic reactions in quartz bearing pelitic rocks. *Contr. Miner. Petrol.* **20**, 244–267.

Ghent, E. D. & Stout, M. Z. 1981. Geobarometry and geothermometry of plagioclase–biotite–garnet–muscovite assemblages. *Contr. Miner. Petrol.* **76**, 92–97.

González-Lodeiro, F. 1983. La estructura del antiforme del Ollo de Sapo. In: *Geología de España, Libro Jubilar J. M. Ríos I* (edited by Comba, J. A.). *Instituto Geológico y Minero de España*, Madrid, Spain.

González-Lodeiro, F., Fernández-Urroz, J., Klein, E., Martínez-Catalán, J. R. & Pablo-Macia, J. G. 1982. Geological Map of Spain S: 1:200,000, Sheet No 8: Lugo. *Instituto Geológico y Minero de España*, Madrid, Spain.

Hodges, K. V. & Spear, F. S. 1982. Geothermometry , geobarometry and the Al_2SiO_5 triple point at Mt Moonsilauke, New Hampshire. *Am. Miner.* **67**, 1118–1134.

Martínez, F. J., Julivert, M., Sebastián, A., Arboleya, M. L. & Gil Ibarguchi, J. I. 1988. Structural and thermal evolution of high-grade areas in the Northwestern parts of the Iberian massif. *Am. J. Sci.* **288**, 969–996.

Martínez, F. J. & Rôlet, J. 1988. Structural and thermal evolution of high-grade areas in the Northwestern parts of the Iberian massif. In: *The Caledonian–Appalachian Orogen* (edited by Harris, A. L. & Fettes, D. J.). *Spec. Publ. Geol. Soc. Lond.* **38**, 611–620.

Martínez-Catalán, J. R. 1985. Estratigrafía y estructura del Domo de Lugo (Sector Oeste de la zona Asturoccidental–leonesa). *Corp. geol. Gall. Sec. Ser.* **II**, 1–191. La Coruña, Spain.

Matte, Ph. 1968. La structure de la virgation hercynienne de Galice (Espagne). *Geol. Alp.* **44**, 155–280.

Olhoeft, G. R. & Johnson, G. J. 1989. Densities of Rocks and Minerals. In: *Practical Handbook of Physical Properties of Rocks and Minerals* (edited by Carmichael, R. S.). CRC Press, Boca Raton, Florida, 139–176.

Parga-Pondal, I., Matte, Ph. & Capdevila, R. 1964. Introduction à la Géologie de l'Ollo de Sapo, formation porphyroide antesilurienne du Nord-Oest de l'Espagne. *Notas y Comunicados del Instituto Geológico y Minero de España, Instituto Geológico y Minero de España* 76, Madrid, Spain. 119–153.

Ponce de León, M. & Choukroune, P. 1980. Shear zones in the Iberian Arc. *J. Struct. Geol.* **2**, 63–68.

Ponce de León, M. & Ribeiro, A. 1981. Position stratigraphique de la formation "Ollo de Sapo" dans la région de Zamora (Espagne)–Miranda do Douro (Portugal). *Commun. Serv. Geol. Portugal* **67**, 141–146.

Rathore, J. S., Courrioux, G. & Choukroune, P. 1983. Study of ductily shear zones (Galicia, Spain) using texture goniometry and magnetic fabric methods. In: *Paleomagnetism of Orogenic Belts* (edited by McClelland Brown, E. & Van den Berg, J.). *Tectonophysics* **98**, 87–109.

Spear, F. S. 1993. Metamorphic phase equilibria and pressure–temperature–time paths. *Min. Soc. Am. Monogr.*, Washington, 1–799.

Spear, F. S. & Cheney, J. T. 1989. A petrogenetic grid for pelitic schists in the system SiO_2–Al_2O_3–FeO–MgO–K_2O–H_2O. *Contr. Miner. Petrol.* **101**, 149–164.